Phys Chem Minerals (2005) 31: 714–720
DOI 10.1007/s00269-004-0434-7

ORIGINAL PAPER

Geraldo Magela da Costa · Ricardo Scholz
Joachim Karfunkel · Vladimir Bermanec
Mário Luiz de Sá Carneiro Chaves

^{57}Fe-Mössbauer spectroscopy on natural eosphorite-childrenite-ernstite samples

Received: 13 February 2004 / Accepted: 16 April 2004 / Published online: 2 February 2005

Abstract Samples of the eosphorite-childrenite [$(Mn^{2+}, Fe^{2+})AlPO_4(OH)_2H_2O$] series from Divino das Laranjeiras and Araçuaí (Minas Gerais State) and Parelhas (Rio Grande do Norte State) pegmatites have been investigated by X-ray diffraction, microprobe analysis and Mössbauer spectroscopy at 295 and 77 K. The Mössbauer spectra of ernstite [$(Mn^{2+}, Fe^{3+})AlPO_4(OH)_{2-x}O_x$] showed the existence of ferric ions in both A and B sites, whereas ferrous ions seem to be located exclusively in the A site. Nonoxidised samples show ferrous ions located in both sites, and no Fe^{3+} could be detected. The interpretation of the Mössbauer spectra of both, oxidised and nonoxidised samples, is difficult because the hyperfine parameters of these minerals are rather similar, rendering it difficult to make proper site assignments.

Keywords Eosphorite · Childrenite · Ernstite · Pegmatite · Mössbauer spectra · Brazil

Introduction

Eosphorite and childrenite, Mn^{2+} $AlPO_4(OH)_2{\cdot}H_2O$ and Fe^{2+} $AlPO_4(OH)_2{\cdot}H_2O$ respectively, are the end-members of a $ABPO_4(OH)_2{\cdot}H_2O$ (A: Mn, Fe; B: Al, Fe) series in which site occupancies of metal cations are still doubtful. The crystal structure of these two closely related minerals is solved in the space groups *Bbam* and *Bba2*, respectively (Barnes 1949; Hanson 1960). The Al octahedron contains two oxygen ions, two OH groups and two water molecules, whereas the more distorted (Mn, Fe) octahedron contains four oxygen ions and two OH groups (Barnes 1949; Hanson 1960; Hoyos et al. 1993). The arrangement of these two octahedra, as well as some interionic distances, is shown in Fig. 1. The Al–O distances are closer to 1.9 Å, whereas the (Mn, Fe) distances are larger at about 0.4 Å. It is generally accepted in the literature that only Fe^{2+} is present in the structure of eosphorite or in intermediate members, although Braithwaite and Cooper (1982) reported that in some Devonshire childrenites Fe^{3+} exceeds Fe^{2+} and suggest that the presence of Fe^{3+} is possibly a result of supergenic oxidation (Bermanec et al. 1995).

Another closely related mineral is ernstite, $(Mn^{2+}, Fe^{3+})AlPO_4(OH)_{2-x}O_x$, which was considered to be formed by oxidation or alteration of eosphorite (Seeliger and Mücke 1970). The crystal structure of this mineral was proposed by these authors on the basis of powder X-ray diffraction, and therefore, single-crystal studies are still needed to confirm the proposed structure.

The distinction between these three minerals is difficult because their X-ray diffraction patterns are similar, especially those of the isomorphous series childrenite and eosphorite. These minerals are frequently found together with other phosphates (e.g. fluorapatite) and silicates (e.g. albite), which in addition makes X-ray identification more difficult. Eosphorite occurs sometimes as larger crystals of gemmological quality, and faceted stones up to 12 ct have been reported, several with typical, syngenetic inclusions (Karfunkel et al. 1997).

Mössbauer spectroscopy is an important technique that can give valuable informations about the iron coordination, occupancy and oxidation state (Bancroft 1973). To our knowledge, only one paper has been published that deals with the Mössbauer spectra of childrenite (Alves

G. M. da Costa (✉)
Departamento de Química,
Universidade Federal de Ouro Preto,
Campus Universitário- Morro do Cruzeiro,
35400 Ouro Preto, MG, Brazil
E-mail: magela@iceb.ufop.br
Tel.: +55-31-35591605

R. Scholz · J. Karfunkel · M. L. de Sá Carneiro Chaves
Departamento de Geologia,
Universidade Federal de Minas Gerais,
31270-901 Belo Horizonte, MG, Brazil

V. Bermanec
Mineralogy and Petrology Institute,
Faculty of Sciences and Mathematics,
University of Zagreb, Zagreb, Croatia

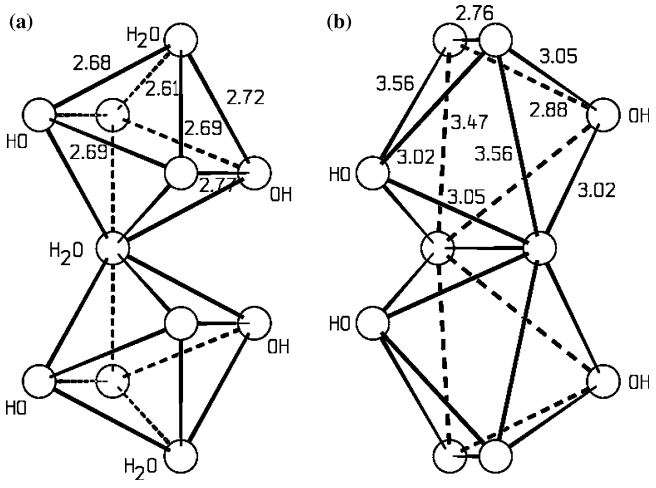

Fig. 1 Perspective view of the aluminum (**a**) and manganese (**b**) octahedra of eosphorite. Interionic distances are given in *Angstroms*

et al. 1980). Unfortunately, no information concerning the composition or the origin of the sample was given. The room-temperature Mössbauer spectrum showed the presence of a narrow, almost symmetrical doublet ($\Delta E_Q = 1.73$ mm/s, $\delta = 1.24$ mm/s) which was attributed to Fe^{2+} linked to the phosphate octahedron.

The present paper is a report of systematic Mössbauer studies of several pegmatite samples from the states of Minas Gerais and Rio Grande do Norte (Brazil), aiming to investigate the process of oxidation and position of M^{3+} cations in the crystal structure of these minerals.

Location

The specimens studied in this work have been sampled from pegmatitic bodies from three different locations: Divino das Laranjeiras and Araçuaí in the Minas Gerais State and Parelhas in the Rio Grande do Norte State.

The Divino das Laranjeiras region is situated 65 km ENE of Governador Valadares and approximately 380 km from Belo Horizonte, the state's capital. More than 60 pegmatites are known to occur in this area, distributed at quadrangle of 400 km^2, some of which are rich in eosphorite, childrenite and ernstite (Scholz et al. 2001). The Lavra da Ilha (Island) pegmatite located near the small village called Taquaral, north of the town Araçuaí, was an important childrenite and eosphorite occurrence in the 1970 decade (Cassedanne and Cassedanne 1973), today only with sporadic activities. The pegmatite is located on an island of the Jequitinhonha River.

The Alto Redondo Pegmatite is located 23 km SE of the town Parelhas, in the south of the Rio Grande do Norte State. Alto Redondo denotes "high round". Many pegmatites in this region are more resistant to weathering processes, overlooking the morphological lower lying surrounding schists.

Experimental

Nine samples were collected from five pegmatitic bodies from Divino das Laranjeiras (three pegmatites), Araçuaí (one pegmatite) and Parelhas (one pegmatite). They were gently crushed and the associated minerals (Table 1) were removed under an optical microscopy.

Powder X-ray diffractograms (XRD) were obtained with a Shimadzu XRD-6000 diffractrometer equipped with a Co-tube and an iron filter. The scanning was done from 13° to 70° (2θ) at 0.25° per min using silicon as internal standard. Cell parameters were calculated by least-squares refinement after subtracting the background and the $K_{\alpha 2}$ contribution and using intensity and angular weighting of the most intense peaks.

Microprobe analysis was done for some selected elements in about 20 spots using a Jeol JXA8900R electron microscope. The following standards were used: Al: AN100, Fe: Olivin, Mn: Rodonite, P: Apatite Artimex, Ca: Apatite Artimex, Na: Albite and Mg: Olivin. These results, along with the brief description of each sample, are given in Table 1. Water contents were calculated from the losses of mass observed at about 450°C in the thermogravimetric analysis (Bermanec et al. 1995).

Mössbauer spectra (MS) were collected at room temperature and 77 K with a spectrometer using a constant-acceleration drive with triangular reference signal, 1,024 channels and in the velocity range of −11 to +11 mm/s (increment of 0.045 mm/s) or −4 to +4 (increment of 0.016 mm/s), respectively. Velocity calibration was achieved from the MS of a standard α-Fe foil at RT, and the isomer shifts are quoted relative to α-Fe. The spectra were fitted either with discrete Lorentzian doublets or with one or two model-independent quadrupole-splitting distributions (Vandenberghe et al. 1994). The range of ΔE_Q for the ferric component was chosen to be between 0.20 mm/s and 2.50 mm/s (steps of 0.10 mm/s), whereas for the ferrous doublet, the range was from 1.30 mm/s to 2.50 mm/s (steps of 0.10 mm/s). Site occupancies by Fe were obtained from the relative areas of the respective subspectra, considering that the recoilless fraction of ferrous ion is 0.9 of that of the ferric component (De Grave and Van Alboom 1991). One problem encountered when quadrupole-splitting distributions are used is that the derived profiles often show small contributions that can be just mathematical artefacts caused by the fitting procedure (Vandenberghe et al. 1994). For this reason we did not consider any contribution accounting for less than 5% of the total spectral area.

Results and discussion

Four representative XRD patterns are displayed in Fig. 2, whereas the calculated cell parameters and the phase identification for all samples are given in Table 2. For most samples, all diffraction lines could be ascribed

Table 1 Chemical analysis (weight %) of childrenite, eosphorite and ernstite

Sample/ pegmatite	AR-01 Alto Redondo		RO-02 Roberto		Li-02 Lavra da Ilha		PI-06 Piano	PI-08 Piano		JF-06 João Firmino		PI-01 Piano		PI-10 Piano		RO-06 Roberto	
Sample description	Yellowish brown to brown color associated to fluorapatite		Pink color associated to hydroxyl-herderite, fluorapatite and siderite		Reddish brown color associated to zanazziite and hydroxyl-herderite		Reddish brown color	Alteration cover with deep brown color and yellowish brown core		Alterated crystal with deep brown color		Reddish brown color with alteration cover		Reddish brown color		Pink color associated to hydroxyl-herderite	
	%	Number of cations	%	Number of cations	%	Number of cations	%	%	Number of cations	%	Number of cations	%	Number of cations	%	Number of cations	%	Number of cations
P_2O_5	33.22	1.03	31.94	1.02	33.17	1.03	32.45	31.91	1.00	32.65	1.04	33.26	1.04	32.84	1.05	32.45	1.05
MnO	14.33	0.45	17.77	0.57	10.66	0.33	21.18	14.56	0.46	14.28	0.46	21.55	0.67	19.95	0.64	16.32	0.53
CaO	0.50	0.02	0.44	0.02	6.02	0.24	0.33	0.39	0.02	2.35	0.10	0.76	0.03	0.32	0.01	0.70	0.03
Na_2O	0.00	0.00	0.01	0.00	0.02	0.00	0.02	0.16	0.01	0.00	0.00	0.00	0.00	0.00	0.00	0.00	0.00
FeO	14.03	0.43	10.52	0.34	10.33	0.32	6.96	5.75	0.18	4.05	0.13	2.49	0.08	8.66	0.27	12.00	0.38
Fe_2O_3	1.22	0.03	0.00	0.00	1.54	0.04	1.53	9.60	0.27	8.69	0.25	4.53	0.13	0.00	0.00	0.00	0.00
MgO	0.35	0.02	0.33	0.02	1.26	0.07	0.08	0.11	0.01	0.25	0.11	0.04	0.00	0.10	0.01	0.27	0.02
Al_2O_3	25.06	1.09	22.23	0.99	23.62	1.02	24.17	23.58	1.03	23.73	1.06	23.34	1.02	23.43	1.05	23.68	1.07
H_2O	15.00	3.67	15.30	3.91	15.20	3.73	14.40	14.40	3.61	13.90	3.50	15.50	3.82	14.80	3.74	14.40	3.66
Total	103.72	6.74	98.54	6.90	101.83	6.78	101.13	100.51	6.63	99.90	6.53	101.47	6.78	100.10	6.77	99.82	6.73

Fig. 2 Powder X-ray diffraction patterns of ernstite and eosphorite (JF06 and PI-08) and "pure" eosphorite (LI-02 and RO-02)

to the above-mentioned minerals. However, for those samples containing ernstite, there is a small peak located at 2.36 Å ($\sim$ 44.5°) that does not belong to either ernstite or EOS. Attempts to identify the origin for this peak were unsuccessful and no further attention will be given to this peak. Although these diffractograms look very similar to each other, it seems that sample JF-06 contains much less EOS than sample PI-08. Simulated diffractograms based on the data contained in the JCPDF files (eosphorite 36-0402; childrenite 11-0621; ernstite 24-0730) are shown in Fig. 3. These X-ray patterns were simulated using a Pearson VII function, line width of 0.10° and Co Kα radiation.

As mentioned before, eosphorite, childrenite and ernstite, all have a very similar XRD pattern, which renders it difficult to distinguish one from the other. In addition, intermediate members are likely to have the same crystallographic structure, which makes the problem even more complex because the peaks will be shifted depending on the composition. The most intense peaks of eosphorite and childrenite almost completely overlap (Fig. 3), a situation that tends to worsen for natural samples presenting a broader linewidth. There are only three peaks, one for eosphorite and two for childrenite,

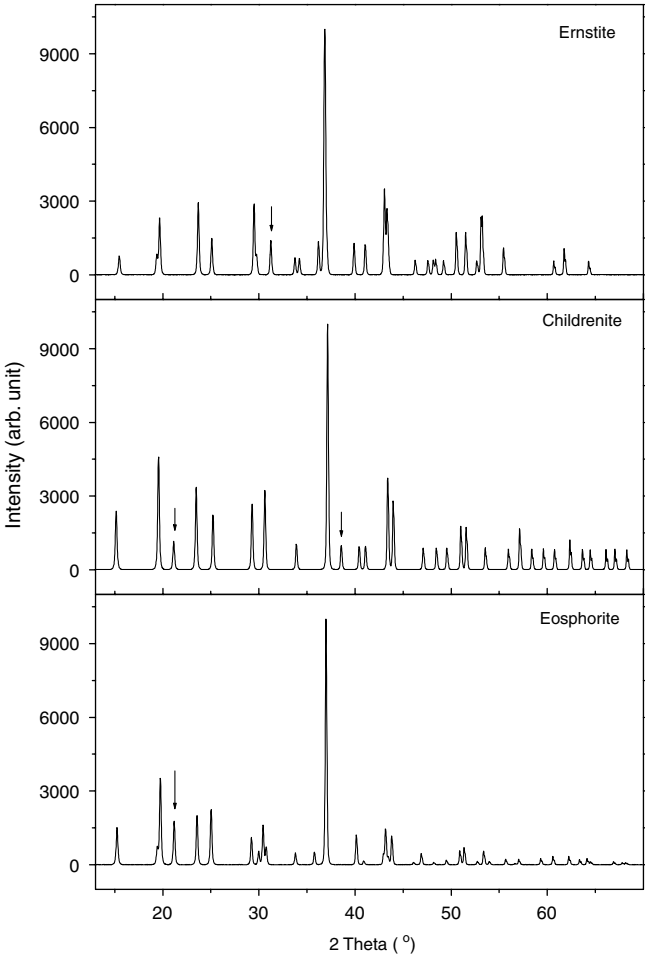

Fig. 3 Simulated X-ray diffraction patterns of ernstite, childrenite and eosphorite. *Arrows* point to "diagnostic" peaks

that could be considered as "diagnostic" peaks, but they are of low intensity and might not be seen. In the case of eosphorite and ernstite, the distinction is not so difficult because the former has an intense peak near 21° (2θ). Thus, eosphorite and childrenite cannot be easily distinguished one from the other by XRD, but if no peak near 21° is present, the sample is close to being single-phase ernstite. As there are no reports in the literature of texture effects on these minerals, the above reasoning must be considered with some caution. In the following discussion, the term "EOS" will be used to represent either eosphorite or childrenite.

The phase identification given in Table 2 was based on the above discussion, and the unit-cell parameters were calculated considering the existence of EOS (RO-06, PI-10, RO-02, AR-PB-01 and LI-02), and an admixture of EOS and ernstite (PI-08, PI-06, PI-01 and JF-06). No systematic variation of the cell parameters with the composition could be deduced.

The room temperature and 77 K Mössbauer spectra of the four samples referred to in Fig. 2 are shown on the left side of Figs. 4, 5, 6, 7. The plots on the right show the probability distributions (dots) obtained from

Table 2 Cell parameters (Å) and phase identification of the studied samples

Sample	*a*	*b*	*c*	Mineral
RO-02	10.429 (3)	13.474 (2)	6.925 (2)	Eosphorite
Li-02	10.434 (3)	13.499 (4)	6.930 (3)	Eosphorite
RO-06	10.393 (6)	13.472 (6)	6.970 (8)	Eosphorite
AR-01	10.428 (6)	13.439 (8)	6.939 (5)	Eosphorite
PI-10	10.430 (2)	13.473 (3)	6.925 (2)	Eosphorite
PI-06	10.411 (7)	13.498 (3)	6.929 (4)	Eosphorite
	13.33 (1)	10.451 (6)	6.974 (4)	Ernstite
PI-01	10.435 (2)	13.504 (7)	6.935 (3)	Eosphorite
	13.29 (1)	10.51 (1)	6.951 (7)	Ernstite
PI-08	10.410 (9)	13.50 (1)	6.960 (5)	Eosphorite
	13.26 (1)	10.431 (7)	6.989 (6)	Ernstite
JF-06	13.281 (8)	10.456 (7)	6.985 (7)	Ernstite
	10.440 (5)	13.50 (2)	6.945 (5)	Eosphorite

fitting the spectra with one or two quadrupole splitting distributions. The solid lines are the adjusted Gaussian curves. The numerical results derived from the fits are listed in Table 3.

The room-temperature MS of sample RO-02 (Fig. 4a) shows only one almost symmetrical doublet that could be well fitted using one discrete Lorentzian component with $\Delta E_Q = 1.74$ mm/s and linewidth of 0.33 mm/s. For the sake of comparison, a fit with one QSD was also performed, and the results are essentially the same as those from the one-doublet fit. The RT spectra of samples RO-06 and PI-10 are similar to that of RO-02. According to the XRD results, all these samples consist of EOS. The 77 K spectrum of RO-02 (Fig. 4b) is apparently also composed of one doublet, but a fit with one discrete Lorentzian doublet resulted in a linewidth of 0.42 mm/s, suggesting the existence of more than one component. Indeed, the use of one quadrupole-splitting distribution improves the fit, and the probability distribution could be well adjusted with two components with $\Delta E_Q = 1.91$ mm/s and

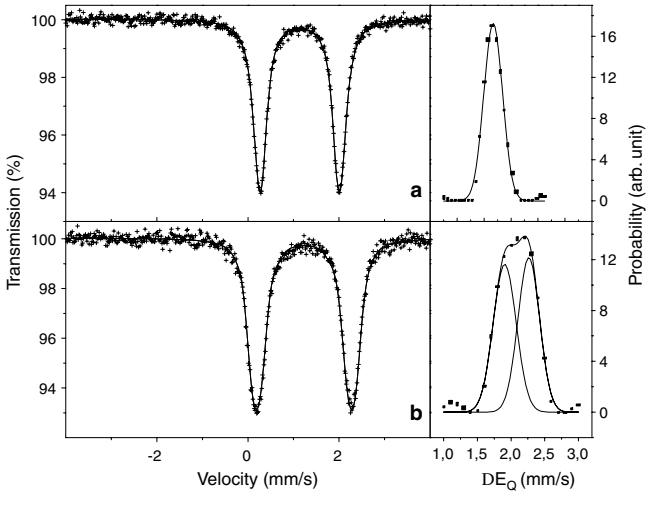

Fig. 4 Mössbauer spectra of sample RO-02 (*left*) and derived probability distributions of quadrupole splittings (*right*): **a** 295 K and **b** 77 K

Table 3 Mössbauer parameters derived from the room temperature and 77 K spectra

Sample	$T(K)$	ΔE_{Q1}	δ_1	S_1	ΔE_{Q2}	δ_2	S_2	ΔE_{Q3}	δ_3	S_3	ΔE_{Q4}	δ_4	S_4
R0-02	RT	1.74	1.25	100									
	77	1.91	1.35	50	2.26	1.35	50						
Li-02	RT	1.70	1.25	87				1.1	0.41	13			
	77	1.92	1.37	30	2.28	1.37	60	1.1	0.46	10			
RO-06	RT	1.73	1.25	100									
AR-01	RT	1.70	1.25	92				1.0	0.41	8			
PI-10	RT	1.74	1.25	100									
PI-06	RT	1.80	1.25	82				1.13	0.41	18			
PI-01	RT	1.70	1.26	35				1.37	0.43	47	0.62	0.43	18
PI-08	RT	1.70	1.25	37				1.36	0.41	54	0.70	0.41	9
	77	–	–	–	2.14	1.36	39	1.49	0.50	41	0.88	0.50	20
JF-06	RT	1.70	1.25	26				1.44	0.42	53	0.76	0.42	21
	77[a]	–	–	–	2.25	1.33	25	1.36	0.49	55			

ΔE_Q is the quadrupole splitting of maximum probability (mm/s), δ is the isomer shift relative to α-Fe (mm/s) and S is the relative area (%)
[a] Sextet component: $H_{hf} = 484$ kOe, $\delta = 0.45$ mm/s; $2\varepsilon_Q = -0.24$ mm/s, $S = 20\%$

$\Delta E_Q = 2.26$ mm/s, respectively, and each with relative areas of 50% (Table 3). It is important to mention that no evidence for the presence of a ferric contribution was found. For Fe^{2+}, a large distortion generally causes the quadrupole splitting to decrease and to become less temperature dependent (Bancroft 1973). Hence, we propose that the doublet with $\Delta E_Q = 1.91$ mm/s (77 K) is due to substitution in the manganese site, whereas the other doublet is due to iron in the aluminum site, and the formula for this EOS could then be written as: $(Mn^{2+}, Fe^{2+})(Al^{3+}, Fe^{2+})PO_4(OH)_2.H_2O$. In order to obtain a charge balance some aluminum sites must be vacant, and therefore the above suggestion must be further investigated. The fact that only one doublet was observed at RT might be explained by the similar values of both isomer shifts and quadrupole-splittings, which however, show different temperature dependencies (Eeckhout et al. 2000).

The room-temperature spectrum of JF-06, which is a mixture of ernstite and EOS, could be successfully fitted, as far as reproducing of the experimental data is concerned, as a superposition of two quadrupole-splitting distributions (Fig. 5a). The probability-distribution plot for the outer doublet is rather narrow, and the high value for the isomer shift (1.25 mm/s) suggests the presence of only one ferrous component accounting for 26% of the spectral area. However, for the inner doublet, the obtained distribution profile clearly shows two contributions with different quadrupole splitting (1.44 and 0.76 mm/s) and the same isomer shift, which is typical for Fe^{3+} in high spin state. The central portion of the 77 K spectrum in the same velocity region (Fig. 5b) is similar to the RT spectrum, but it shows a small peak near −4 mm/s, indicating the presence of a magnetic component. The MS at 77 K collected at a larger velocity scale is displayed in Fig. 5c and clearly shows the presence of the sextet component accounting for about 20% of the spectral area and whose hyperfine parameters ($H_{hf} = 484$ kOe, $\delta = 0.45$ mm/s and $2\varepsilon_Q = -0.24$ mm/s) are consistent with those of goethite containing at least 20 mol% of aluminum (Fysh and Clark 1982; Murad and Johnston 1987). This sextet is not seen at room temperature because the aluminum substitution causes a collapse of the magnetic ordering, and in this case the MS of goethite consists of a doublet with a quadrupole splitting of ~0.6 mm/s (Murad and Johnston 1987). It is relevant to mention that the relative area of the doublet with average $\Delta E_Q = 0.76$ mm/s seen in the RT spectrum (Fig. 5a) is quite close to that of the sextet, which gives additional support to the above interpretation. The distribution plot for the ferric component at 77 K is very broad and it is centred at 1.36 mm/s, whereas for the ferrous component the maxima is located at 2.25 mm/s. The 77 K Mössbauer spectrum obtained on the velocity scale (±4 mm/s, Fig. 5b) was fitted including one sextet component with all parameters fixed at the values derived from the MS obtained on the velocity scale (±11 mm/s, Fig. 5c). Two additional QSD were used to account for the ferric and ferrous contributions, and the results are essentially the same as those obtained from the spectrum shown in Fig. 5c. The next question to be answered concerns the

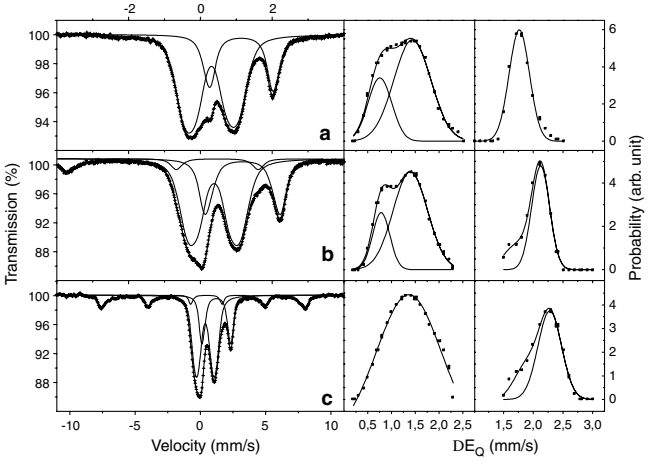

Fig. 5 Mössbauer spectra of sample JF-06 (*left*) and derived probability distributions of quadrupole splittings (*right*): **a** 295 K, **b** and **c** 77 K. Note that the velocity scale for the **a** and **b** is ~4 mm/s, whereas for **c** is ~11 mm/s

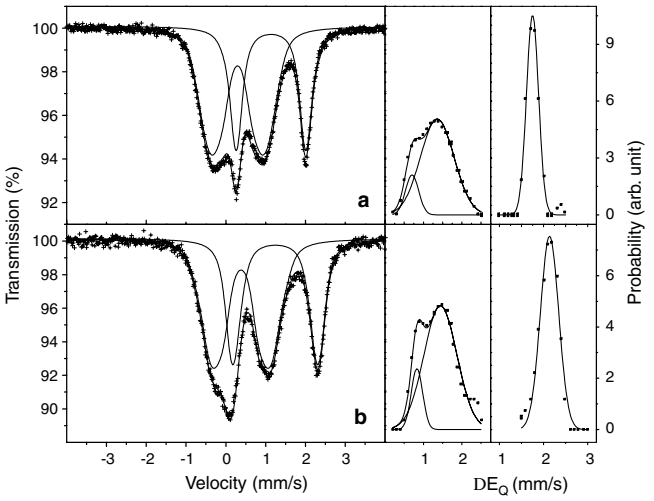

Fig. 6 Mössbauer spectra of sample PI-08 (*left*) and derived probability distributions of quadrupole splittings (*right*): **a** 295 K and **b** 77 K

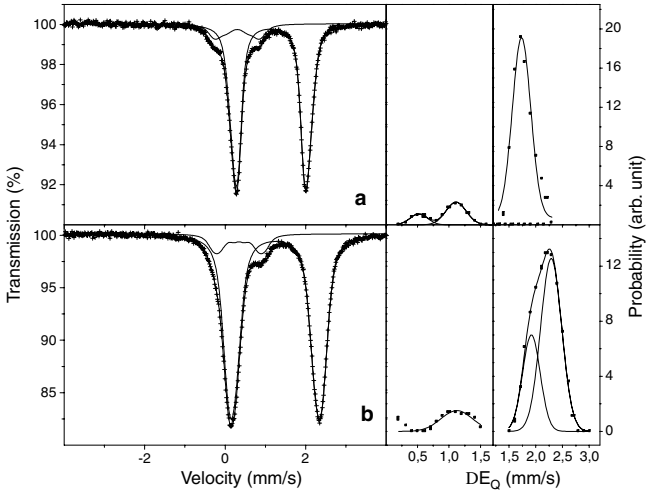

Fig. 7 Mössbauer spectra of sample LI-02 (*left*) and derived probability distributions of quadrupole splittings (*right*): **a** 295 K and **b** 77 K

partition of the iron ion into the structure of ernstite in sample JF-06. Assuming that ernstite is formed by oxidation of EOS, it seems reasonable to propose that the ferrous ions are located in the manganese site. The bimodal distribution profile for Fe^{3+} could mean that both sites are occupied. In that case, the general formula can be written as: $(Mn^{2+}, Fe^{2+}, Fe^{3+})(Al^{3+}, Fe^{3+})$-$PO_4(OH)_{2-x}O_x$. Another plausible explanation is that the ferrous ions are exclusively due to EOS, and therefore ernstite would only contain Fe^{3+}. However, as the XRD pattern shows EOS as a minor phase, the first interpretation seems to be more likely.

Sample PI-08 also contains ernstite and EOS (see Table 2). The RT and 77 K Mössbauer spectra (Fig. 6a, b, respectively) resemble that of JF-06: the ferric doublet is quite broad, whereas the ferrous doublet is narrow and more intense for PI-08. These spectra were fitted using the same procedure as described for JF-06, and the numerical results derived from the fits are listed in Table 3. It is important to mention that the 77 K spectrum for this sample does not show the sextet seen for JF-06, and thus the two Fe^{3+} contributions revealed in the distribution plots are certainly due to iron ions in the structure of both ernstite and/or EOS. The results for RO-02 showed the absence of ferric ions in the structure of EOS, and thus it seems reasonable to assume that all Fe^{3+} in PI-08 is due to ernstite. On the other hand, the ferrous doublet can be due to any of these two minerals, and as the hyperfine parameters are very similar for both of them (Table 3), it is not possible to resolve the respective subspectra.

The last sample to be discussed is LI-02, which supposedly only contains EOS (Table 2). The RT and 77 K Mössbauer spectra (Fig. 7a, b) show an intense and relatively narrow Fe^{2+} doublet, with a weak and broad Fe^{3+} contribution (~10%) superimposed to the low-velocity Fe^{2+} peak. The distribution plot for the ferrous doublet obtained from the 77 K MS shows two contributions with $\Delta E_Q = 1.92$ mm/s and $\Delta E_Q = 2.28$ mm/s, which are practically the same as those obtained for RO-02. Thus, it seems coherent to propose that the ferrous doublets are due to EOS and that the ferric contribution is due to the presence of small quantities of ernstite.

In conclusion, this work has shown that the identification of eosphorite, childrenite and ernstite is not so straightforward as claimed in literature, and that the existence of solid solutions or mixtures can only be confirmed after an exhaustive characterisation.

Acknowledgements This work was partially supported by CNPq and Fapemig (Brazil), and by the Ministry of Science and Technology of Croatia (Project No. 0119420). The plot of the crystallographic structure of eosphorite was kindly prepared by Dr. Genivaldo Júlio Perpétuo (Physics Department, UFOP).

References

Alves KMB, Garg R, Garg VK (1980) A Mössbauer resonance study of Brazilian childrenite. Radiochem Radioanal Lett 45:129–132

Bancroft GM (1973) Mössbauer spectroscopy: an introduction for inorganic chemists and geochemists. Wiley, New York, 252 p

Barnes WH (1949) The unit cell and space group of childrenite. Am Mineral 34:12–18

Bermanec V, Šćavničar S, Zebec V (1995) Childrenite and crandallite from the Stari Trg mine (Trepča), Kosovo: new data. Mineral Petrol 52:197–208

Braithwaite RSW, Cooper BV (1982) Childrenite in South-West England. Mineral Mag 46:119–126

Cassedanne JP, Cassedanne J (1973) Minerals from the Lavra da Ilha pegmatite, Brazil. Mineral Rec 4(5):207–213

De Grave E, Van Alboom A (1991) Evaluation of ferrous and ferric Mössbauer fractions. Phys Chem Miner 18:337–342

Eeckhout SG, De Grave E, McCammon CA, Vochten R (2000) Temperature dependence of the hyperfine parameters of synthetic $P2_1/c$ Mg-Fe clinopyroxenes along the $MgSiO_3$-$FeSiO_3$join. Am Mineral 85:943–952

Fysh SA, Clark PE (1982) Aluminous goethite: a Mössbauer study. Phys Chem Miner 8:180

Hanson AW (1960) The crystal structure of eosphorite. Acta Cryst 13:384–387

Hoyos MA, Calderon T, Vergara I, Garcia-Solé J (1993) New structural and spectroscopic data for eosphorite. Mineral Mag 57:329–336

Karfunkel J, Chaves MLSC, Banko A, Irran E (1997) Ernstite and eosphorite from Minas Gerais, Brazil. Mineral Rec 28(6):489–493

Murad E, Johnston JH (1987) Iron oxides and oxyhydroxides. In: Long GJ (ed) Mossbauer spectroscopy applied to inorganic chemistry. Plenum, New York, pp 507–582

Scholz R, Addad J, Karfunkel J, Martins MS, Bermanec V, Kniewald G, Figueiredo JCD Jr, Souza LAC, Sousa SHB (2001) Caracterização petrogenética e geoquímica de ambligonita-montebrasitas em pegmatitos de Divino das Laranjeiras, Minas Gerais, Brasil. In: 6° Congresso de Geoquímica dos Países de Língua Portuguesa, Anais. Faro, Portugal, pp 88–91

Seeliger Von E, Mücke A (1970) Ernstit, ein neues Mn^{2+}-Fe^{3+}-Al-Phosphate und seine Beziehungen zum Eosphorit. N Jahrb Mineral Monatsh 289–298

Vandenberghe RE, De Grave E, de Bakker PMA (1994) On the methodology of the analysis of Mössbauer spectra. Hyperfine Interactions 83:29–49